

Extended nebular emission in CALIFA early-type galaxies

J.M. Gomes¹, P. Papaderos¹, C. Kehrig², J.M. Vilchez², M.D.
Lehnert³ and the CALIFA collaboration

¹Instituto de Astrofísica e Ciências do Espaço, Universidade do Porto, CAUP, Rua das
Estrelas, PT4150-762 Porto, Portugal

email: jean@astro.up.pt; papaderos@astro.up.pt

²Instituto de Astrofísica de Andalucía (CSIC), Glorieta de la Astronomía s/n Aptdo. 3004,
E18080-Granada, Spain

³Institut d'Astrophysique de Paris, UMR 7095, CNRS, Université Pierre et Marie Curie, 98 bis
boulevard Arago, 75014 Paris, France

Abstract. The morphological, spectroscopic and kinematical properties of the warm interstellar medium (*wim*) in early-type galaxies (ETGs) hold key observational constraints to nuclear activity and the buildup history of these massive quiescent systems. High-quality integral field spectroscopy (IFS) data with a wide spectral and spatial coverage, such as those from the CALIFA survey, offer a precious opportunity for advancing our understanding in this respect. We use deep IFS data from CALIFA (califa.caha.es) to study the *wim* over the entire extent and optical spectral range of 32 nearby ETGs. We find that all ETGs in our sample show faint ($H\alpha$ equivalent width $EW(H\alpha)\sim 0.5 \dots 2 \text{ \AA}$) extranuclear nebular emission extending out to ≥ 2 Petrosian₅₀ radii. Confirming and strengthening our conclusions in Papaderos et al. (2013; hereafter P13) we argue that ETGs span a broad *continuous* sequence with regard to the properties of their *wim*, and they can be roughly subdivided into two characteristic classes. The first one (type i) comprises ETGs with a nearly constant $EW(H\alpha)\sim 1\text{--}3 \text{ \AA}$ in their extranuclear component, in quantitative agreement with (even though, no proof for) the hypothesis of photoionization by the post-AGB stellar component being the main driver of extended *wim* emission. The second class (type ii) consists of virtually *wim*-evacuated ETGs with a large Lyman continuum (L_{yc}) photon escape fraction and a very low ($\leq 0.5 \text{ \AA}$) $EW(H\alpha)$ in their nuclear zone. These two ETG classes appear indistinguishable from one another by their LINER-specific emission-line ratios. Additionally, here we extend the classification by P13 by the class i+ which stands for a subset of type i ETGs with low-level star-forming activity in contiguous spiral-arm like features in their outermost periphery. These faint features, together with traces of localized star formation in several type i&i+ systems point to a non-negligible contribution from young massive stars to the global ionizing photon budget in ETGs. Moreover, our results further highlight the considerable diversity of ETGs with respect to their gaseous and stellar kinematics. Whereas in one half of our sample gas and stars show similar (yet no identical) velocity patterns, both dominated by rotation along the major galaxy axis, our CALIFA data also document several cases of kinematical decoupling or stellar rotation along the minor galaxy axis.

Keywords. galaxies: elliptical and lenticular, cD - galaxies: evolution - galaxies: formation

1. Introduction

Even though the presence of faint nebular emission (*ne*) in the nuclei of many early-type galaxies (ETGs) has long been established observationally (e.g., Sarzi et al. 2010; Kehrig et al. 2012), the nature of the dominant excitation mechanism of the warm interstellar medium (*wim*) in these systems remains a subject of debate. The *low-ionization nuclear emission-line region* (LINER) emission-line ratios, as a typical property of ETG nuclei,

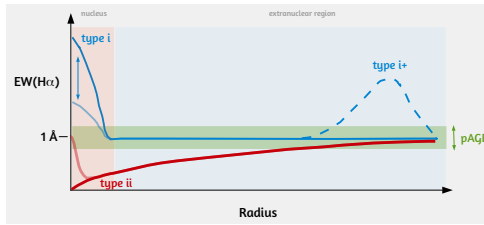


Figure 1. Schematic representation of the two main classes of ETGs, as defined in P13 and G14. The $\text{EW}(\text{H}\alpha)$ profiles of **type i** ETGs show in their extranuclear component nearly constant values within the narrow range between $\sim 0.5 \text{ \AA}$ and $\sim 2.4 \text{ \AA}$, with a mean value of typically $\sim 1 \text{ \AA}$. A few of these systems (labeled **i+**) additionally show an $\text{EW}(\text{H}\alpha)$ excess in their periphery, which, as discussed in G14, is due to low-level star-forming activity. The defining property of **type ii** ETGs is a centrally very low ($\lesssim 0.5 \text{ \AA}$) mean $\text{EW}(\text{H}\alpha)$, increasing then smoothly to $\sim 1 \text{ \AA}$ at their periphery. Regarding their nuclear properties, both ETG types show a large diversity, from systems with virtually *wim*-evacuated cores ($\lesssim 0.1 \text{ \AA}$) to galaxies with a compact nuclear $\text{EW}(\text{H}\alpha)$ excess.

have prompted various interpretations (see, e.g., Yan & Blanton 2012), including low-accretion rate active galactic nuclei (AGN; e.g., Ho 2008), fast shocks (e.g. Dopita & Sutherland 1995), and hot, evolved ($\geq 10^8 \text{ yr}$) post-AGB (pAGB) stars (e.g., Binette et al. 1994; Stasińska et al. 2008). High-quality integral field spectroscopy (IFS) data with a wide spectral and spatial coverage, such as those from the *Calar Alto Legacy Integral Field Area* (CALIFA) survey (Sánchez et al. 2012), offer an important opportunity to gain insight into the nature of nuclear and extranuclear gas excitation sources and advance our understanding on the evolutionary pathways of ETGs. Here we provide a brief summary of our results from an ongoing study of low-spectral-resolution ($R \sim 850$) CALIFA IFS cubes, observed with PMAS/PPAK (Roth et al. 2005; Kelz et al. 2006), for 20 E and 12 S0 nearby ($< 150 \text{ Mpc}$) galaxies. This sample was initially studied in Papaderos et al. (2013; P13) with main focus on the radial distribution of the $\text{EW}(\text{H}\alpha)$ and Lyman continuum photon escape fraction (L_{γ_c}) in ETGs, and has permitted a tentative subdivision of these systems into two main classes. A thorough 2D analysis of the same sample, including, e.g., $\text{EW}(\text{H}\alpha)$ and stellar age maps, stellar and gas kinematics and gas excitation diagnostics will be presented in Gomes et al. (2014; hereafter G14). G14 also provide a detailed description of our IFS data processing and spectral modeling pipeline **Porto3D** and of the methods used to determine the radial distribution of various quantities of interest (e.g., $\text{EW}(\text{H}\alpha)$) both based on single-spaxel (**sisp**) determinations and a statistics analysis of **sisp** measurements within isophotal annuli (**isan**).

2. Results

Figure 1 illustrates on the example of the S0 galaxy NGC 1167 some of the quantities determined and discussed in G14. Panels **a** & **b** show the $\text{H}\alpha$ flux in $10^{-16} \text{ erg s}^{-1} \text{ cm}^{-2}$ (cf vertical bar to the right of the panel) and $\text{EW}(\text{H}\alpha)$ in Å , as determined after subtraction of the best-fitting synthetic stellar spectrum at each spaxel. The radial distribution of these two quantities as a function of the photometric radius R^* (arcsec) is shown in panels **c** and **d**), respectively. **sisp** determinations obtained within the nuclear region, defined as twice the angular resolution of the IFS data (i.e. for $R^* \leq 3.8 \text{ arcsec}$) and in the extranuclear component are shown with red and blue circles, respectively. Open squares correspond to **isan** determinations within irregular isophotal annuli with the vertical bars illustrating the $\pm 1\sigma$ scatter of individual **sisp** measurements.

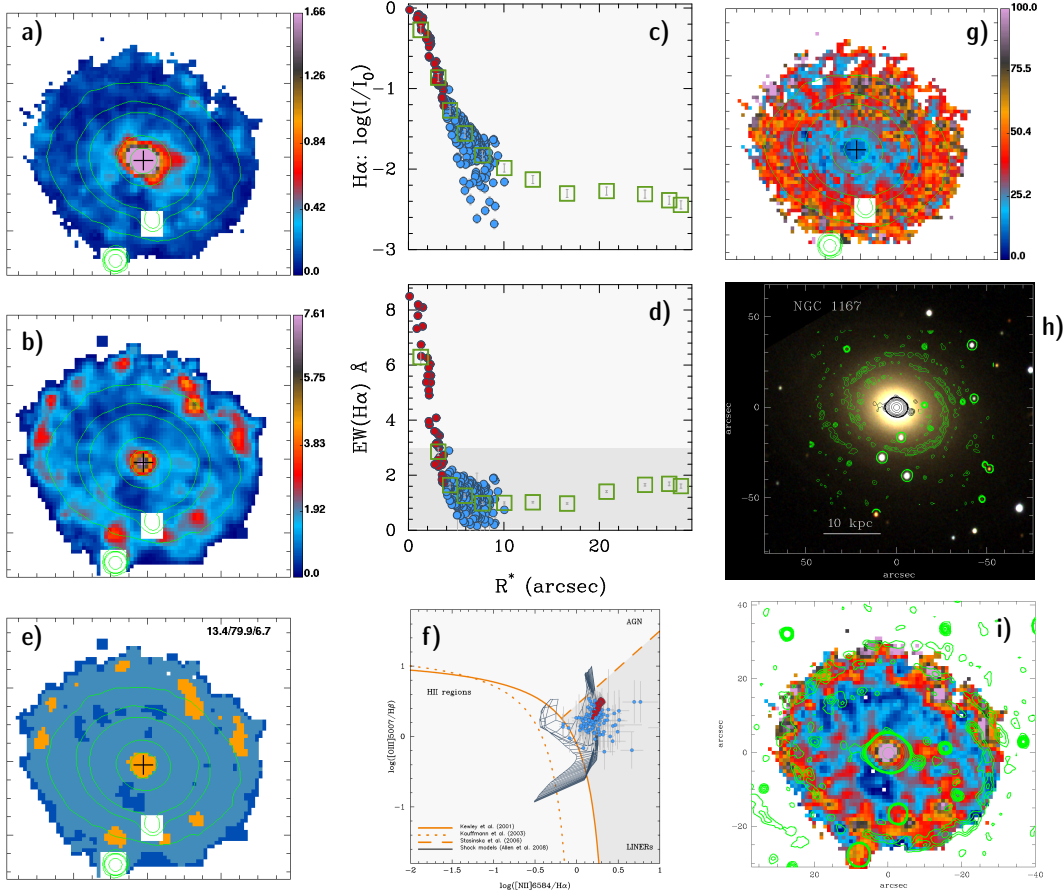


Figure 2. NGC 1167: a–d) $\text{H}\alpha$ and $\text{EW}(\text{H}\alpha)$ maps and radial profiles; e) Diagnostic subdivision of the $\text{EW}(\text{H}\alpha)$ map (see discussion); f) BPT diagram; g) Luminosity contribution of stars younger than 5 Gyr; Contours overlaid with a true-color SDSS image and the $\text{EW}(\text{H}\alpha)$ map (h & i, respectively) depict faint spiral-like features in the periphery of the ETG, as revealed by image processing with an unsharp-masking technique.

A subdivision of the $\text{EW}(\text{H}\alpha)$ map into three intervals (panel e) is meant to help the reader to distinguish between regions where the observed $\text{EW}(\text{H}\alpha)$ is consistent, within the uncertainties, with pure pAGB photoionization ($0.5\text{--}2.4 \text{ \AA}$; light blue), an additional gas excitation source is needed to account for the $\text{EW}(\text{H}\alpha)$ ($\geq 2.4 \text{ \AA}$; yellow), and where the $\text{EW}(\text{H}\alpha)$ is by a factor ≥ 2 lower than that predicted from pAGB photoionization models ($\leq 0.5 \text{ \AA}$; dark blue), hence L_{Y} photon escape is important. The percentage of the spectroscopically studied area that is consistent with these three interpretations is indicated at the upper-right.

Panel f) shows *sisip* and *isan* determinations of the $\log([\text{N II}]_{6583}/\text{H}\alpha)$ vs $\log([\text{O III}]_{5007}/\text{H}\beta)$ diagnostic emission-line ratios after Baldwin et al. (1981, referred to in the following as BPT ratios). The meaning and color coding of the symbols is identical to that in panels c&d. The loci on the BPT diagrams that are characteristic of AGN and LINERs, and that corresponding to photoionization by young massive stars in HII regions are indicated by demarcation lines from Kauffmann et al. (2003, dotted curve), Kewley et al. (2001, solid curve) and Schawinski et al. (2007, dashed line). The grid of thin-gray lines roughly at

the middle of each diagram depicts the parameter space that can be accounted for by pure shock excitation, as predicted by Allen et al. (2008) for a magnetic field of $1 \mu\text{G}$, and a range of shock velocities between 100 and 1000 km s^{-1} , for gas densities between 0.1 and 100 cm^{-3} .

The luminosity contribution $\mathcal{L}_{5 \text{ Gyr}}$ (%) of stars younger than 5 Gyr at the normalization wavelength (panel g) echoes the well established fact that ETGs are dominated by an evolved stellar component throughout their optical extent. Note the clear trend for an outwardly increasing $\mathcal{L}_{5 \text{ Gyr}}$, which is consistent with inside-out galaxy growth, or even the presence of low-level star-forming activity in the galaxy periphery.

The overlaid contours on the true-color SDSS image (panel h) depict faint spiral-like features in the periphery of NGC 1167, as revealed by image processing with the flux-conserving unsharp-masking technique by Papaderos et al. (1998). As apparent from panel i, these contiguous low-surface brightness features are spatially correlated with moderately extended zones of enhanced EW(H α). This indicates that they are not purely stellar relics from fading spiral arms that have long ceased forming stars, but sites of ongoing low-level star formation in the extreme periphery of NGC 1167 (see detailed discussion of this subject in G14).

Acknowledgements

JMG is supported by a Post-Doctoral grant, funded by FCT/MCTES (Portugal) and POPH/FSE (EC) and PP by an FCT Investigador 2013 Contract, funded by FCT/MCTES (Portugal) and POPH/FSE (EC). They acknowledge support by the Fundação para a Ciência e a Tecnologia (FCT) under project FCOMP-01-0124-FEDER-029170 (Reference FCT PTDC/FIS-AST/3214/2012), funded by FCT-MEC (PIDDAC) and FEDER (COMPETE).

References

- Allen, M. G., Groves, B. A., Dopita, M. A. et al. 2008, ApJS, 178, 20
 Baldwin, J. A., Phillips, M. M., & Terlevich, R. 1981, PASP, 93, 5
 Binette, L., Magris, C. G., Stasińska, G., & Bruzual, A. G. 1994, A&A, 292, 13
 Dopita, M. A. & Sutherland, R. S. 1995, ApJ, 455, 468
 Gomes, J.M., Papaderos, P., Kehrig, C., Vílchez, J.M., Lehnert, M.D., Sánchez, S., Ziegler, B. et al. 2014, in prep.
 Ho, L.C. 2008, ARA&A, 46, 475
 Kauffmann, G., Heckman, T. M., Tremonti, C. et al. 2003, MNRAS, 346, 1055
 Kehrig, C., Monreal-Ibero, A., Papaderos, P., et al. 2012, A&A, 540, A11 (K12)
 Kelz, A., Verheijen, M.A.W., Roth, M.M. et al. 2006, PASP, 118, 129
 Kewley, L. J., Dopita, M. A., Sutherland, R. S., Heisler, C. A., Trevena, J. 2001, ApJ, 556, 121
 Papaderos, P., Izotov, Y.I., Fricke, K.J., Thuan, T.X., Guseva, N.G. 1998, A&A, 338, 43
 Papaderos, P., Gomes, J.M., Vílchez, J.M. et al. 2013, A&A, 555, L1
 Roth, M.M., Kelz, A., Fechner, T. et al. 2005, PASP, 117, 620
 Sánchez, S. F., Kennicutt, R. C., Gil de Paz, A., et al. 2012, A&A, 538, A8
 Sánchez, S., Advances in Astronomy, Issue: *Metals in 3D: A Cosmic View from Integral Field Spectroscopy*, 2014a, in press
 Sarzi, M., Shields, J. C., Schawinski, K., et al. 2010, MNRAS, 402, 2187
 Schawinski, K., Thomas, D., Sarzi, M., et al. 2007, MNRAS, 382, 1415
 Stasińska, G., Vale Asari, N., Cid Fernandes, R. et al. 2008, MNRAS, 391, L29
 Trinchieri, G. & di Serego Alighieri, S. 1991, AJ, 101, 1647
 Yan, R. & Blanton, M.R. 2012, ApJ, 747:61